

Electronic state analysis of Li_2RuO_3 positive electrode for lithium ion secondary battery

Masatsugu Oishi*, Ryoshi Imura, Tomoyuki Ueki
*Graduate School of Technology, Industrial and Social Science, Tokushima University,
2-1 Minamijosanjima cho, Tokushima 770-8506, Japan
oishi.masatsugu@tokushima-u.ac.jp*

Keiji Shimoda*
*Office of Society-Academia Collaboration for Innovation, Kyoto University,
Gokasho, Uji, Kyoto 611-0011, Japan
shimoda.keiji.6v@kyoto-u.ac.jp*

Hirona Yamagishi, Iwao Watanabe
*Ritsumeikan University, SR center,
1-1-1 Higashinoji Kusatsu Shiga 525-8577, Japan
iwa-wata@gst.ritsumei.ac.jp*

Received Day Month Day
Revised Day Month Day

An investigation was made on the electronic structure of 4d transition metal layered oxide material of Li_2RuO_3 using X-ray photoelectron spectroscopy (XPS) and X-ray absorption spectroscopy (XAS). The intensity of O *K* pre-edge peak increased for Li ion extracted samples, suggesting increased ligand holes. The Ru 3d XPS spectrum suggested the variation of local structure around Ru ions by extraction of Li ions. We conclude that the delithiation from Li_2RuO_3 is charge-compensated by O anions, and that the creation of the ligand holes reorganizes electronic structures composed of highly hybridized Ru 4d and O 2p orbitals.

Keywords: Lithium ion secondary battery; XAS; XPS; O anion redox reaction

* Corresponding authors.

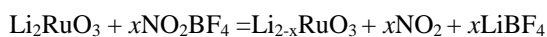
1. Introduction

In a lithium ion secondary battery (LIB), Li ions move back and forth between the electrodes. The cathode materials in practical use for LIB normally keep their crystal structure during the insertion and removal of Li ions. Thus, they exhibit excellent cyclability.¹ In the conventional cathode material of LiCoO_2 , delithiation of more than 0.6 mol causes oxidation of O anions leading to O_2 gas formation and deterioration of the material. Therefore, only about 0.6 mol of Li ions can be reversibly removed and inserted. The useful capacities of LiCoO_2 are then less than the amounts we expect from the chemical formula.¹ Li-rich layered metal oxides have been proposed as potential electrode

materials for the next generation LIBs, which show larger capacities compared to conventional layered metal oxides. Some of Li-rich layered metal oxides contain larger amounts of Li ions which can be reversibly removed and inserted by incorporating redox reactions of not only metal cations but also O anions. We reported the electronic state variations of O anions in the Li_2MnO_3 and $\text{Li}_{1.16}\text{Ni}_{0.15}\text{Co}_{0.19}\text{Mn}_{0.50}\text{O}_2$ positive electrodes by X-ray absorption spectroscopy (XAS).^{2,3} The XAS results of Li_2MnO_3 indicated the participation of O anions, in the form similar to those of superoxides and peroxides, to charge-compensate the Li-ion defects. The contribution of electrons from O 2p levels during the oxidation process differs significantly depending on the constituent metal cations since the degree of the hybridization between metal and O levels influences the electronic state of O anions during the oxidation process. Our previous studies^{2,3} concerning 3d metals such as Li_2MnO_3 are further extended to electrodes containing 4d metals. Here we report on the results of 4d transition metal layered oxide material of Li_2RuO_3 .

2. Experimental

Li_2RuO_3 was prepared by solid phase method using Li_2CO_3 (Wako, 99.0%, Japan) and RuO_2 (Rare Metallic, 99.9%, Japan), and calcined three times with an intermittent grinding at 600°C, 1000°C, and 1200°C for 3 hours.⁴ Li-deficient samples were prepared using a chemical treatment.⁵ The sample powders in acetonitrile were subjected to oxidation treatment using NO_2BF_4 . The degree of delithiation was controlled by adjusting the amounts of the oxidant. The delithiation reaction follows the equation below:



The delithiated powders obtained were filtered and washed repeatedly with distilled water. They were finally dried in a vacuum at 120 °C. The obtained powders were subjected to a composition analysis using inductivity coupled plasma-atomic emission spectrometry (ICP-AES) (ICPS-8100, Shimadzu, Japan). Powder X-ray diffraction (XRD) experiments (Multiflex, Rigaku, Japan) were performed using $\text{CuK}\alpha$ at room temperature. X-ray photoelectron spectroscopy (XPS) spectra were acquired on a photoelectron spectrometer (PHI5000 VersaProbe II, ULVAC-PHI, Japan), with monochromatized Al $K\alpha$ radiation (1486.6 eV) and applying a dual beam charge neutralizer (low energy electrons and Ar^+ ions). The binding energies were calibrated with respect to the C 1s signal at 284.8 eV. The O K -edge XAS spectra were collected at the soft X-ray beam line, BL-11, at the SR Center, Ritsumeikan University (Shiga, Japan). The XAS spectra were simultaneously obtained in both the total electron yield (TEY) mode using a sample drain current and the partial fluorescence X-ray yield (PFY) mode using a silicon drift detector (KETEK, VITUS R100 with a 0.1 μm thick Polyethylene-N film window). The electronic density of states for the ground state structures of Li_2RuO_3 were calculated with CASTEP program package.⁶ We employed GGA+ U ($U = 4.5$ eV for Ru d-orbital).⁷ Ultrasoft pseudopotentials were used and the plane wave cutoff energy was taken to be 380 eV. The convergence parameters were as follows: total energy tolerance: 0.5×10^{-5} eV/atom, maximum force tolerance: 0.01 eV/Å, maximal stress: 0.02 GPa, and maximal displacement: 0.5×10^{-3} Å.

3. Results and Discussion

Figure 1 shows XRD profiles of the pristine and delithiated samples. The contents of Li and Ru metal ions in the materials were determined by ICP-AES. The amounts of delithiation were calculated assuming no loss of Ru ions during the chemical treatments. The diffraction peaks from the pristine state were defined with monoclinic structure of space group $C2/c$.⁸ The XRD profiles of the delithiated samples showed the decrease in the content of the pristine Li_2RuO_3 phase, and increase of the Li-poor phases of $\text{Li}_{1.4}\text{RuO}_3$ with a monoclinic symmetry ($C2/c$) and $\text{Li}_{0.9}\text{RuO}_3$ with a rhombohedral symmetry ($R-3$).^{8,9}

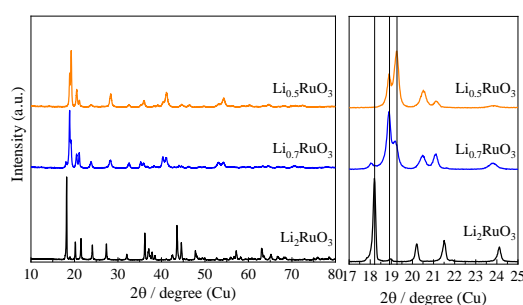


Fig. 1. XRD profiles of $\text{Li}_{2-x}\text{RuO}_3$.

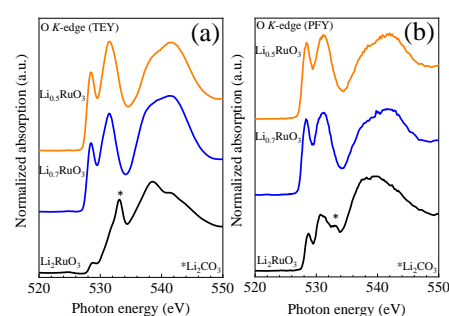


Fig. 2. O K -edge XAS spectra of $\text{Li}_{2-x}\text{RuO}_3$ in (a) TEY and (b) PFY

The O K -edge XAS spectra of $\text{Li}_{2-x}\text{RuO}_3$ are shown in Fig.2. Each spectrum is composed of pre-edge peaks appearing between 528–534 eV and a broad band above 534 eV. The broad band shifted to the higher photon energy for the delithiated samples. The upward shift is associated with shortening of the Ru–O bond distances.¹⁰ The strong peak at 532 eV clearly observed in the surface sensitive TEY mode corresponds to that of Li_2CO_3 , which indicates that the surface was covered by Li_2CO_3 . The PFY mode probes rather deeper part of the particles. Two pre-edge peaks and a Li_2CO_3 peak were recognized for the pristine state. The projected density of states of Li_2RuO_3 showed that the Ru and O bands are highly hybridized around the Fermi level (Fig.3). Two peaks observed in the O K pre-edge region reflect the empty O 2p orbitals above the Fermi level (at 0 eV) which are significantly hybridized with Ru 4d orbitals (t_{2g} , e_g^*). The pre-edge peak intensity increased for the delithiated samples suggesting the formation of hole states in the hybridized bands of Ru4d–O2p.

The strong O 1s peak at 531.5 eV in the XPS data represents the Li_2CO_3 formed on the surface (Fig.4a). The O^{2-} state in the Li_2RuO_3 crystal lattice was observed as a shoulder peak at 529.3 eV. The C 1s peaks assigned to C–C bonds and carbonates, CO_3^{2-} , were also observed in the pristine sample (Fig.4b). The intensities of these peaks decreased after the chemical delithiation. The Ru 3d_{5/2} and 3d_{3/2} XPS for $\text{Li}_{0.7}\text{RuO}_3$ were similar to those for Li_2RuO_3 but the peaks for $\text{Li}_{0.5}\text{RuO}_3$ shifted to lower energy (Fig.4b). Ru L -edge XAS spectra for a Li_2RuO_3 electrode system were studied by Mori *et al.*¹¹ They found that Ru^{4+} ions were oxidized to Ru^{5+} at 4.2 V vs. Li^+/Li^0 . They also found that further oxidation to 4.8 V induced negative peak shifts. They explained this phenomenon as a variation of the

RuO₆ octahedral symmetry associated with the phase transition during delithiation, but not as the reduction of Ru ions. Moreover, the reductive shifts in the Ru 3d peak energies were reported for Ru-based Li₂(Ru, M)O₃ (M=Sn, Mn, Ti) materials.^{12,13} These were explained as a result of reorganization of Ru4d–O2p covalent bonding states caused by the anionic oxidation that creates unstable oxygen ligand holes in the oxygen network. The present O 1s XPS spectra for Li ion extracted samples showed a new peak at around 530.5 eV (Fig.4a), being at higher binding energy than 529.3 eV (O²⁻ in the crystal lattice), which may suggest the oxidized O anions as reported by Tarascon's group.¹³

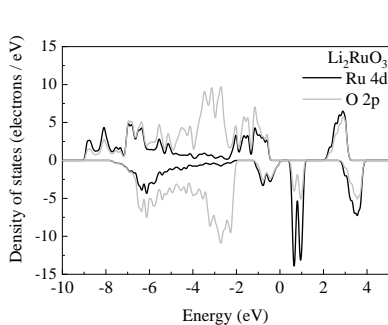


Fig. 3. Projected density of states of Li₂RuO₃.

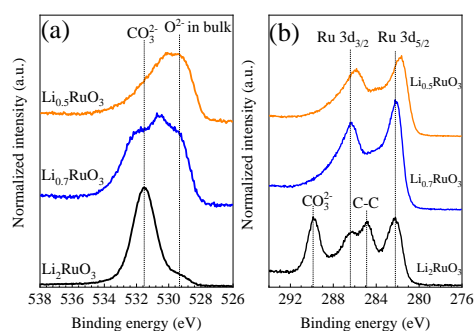


Fig. 4. (a) O 1s and (b) Ru 3d and C 1s XPS spectra of Li_{2-x}RuO₃.

3. Conclusion

We observed the electronic structure variations for Li₂RuO₃ in the delithiation process by using XAS and XPS. The increased pre-edge peak intensities in the O K-edge XAS spectra for the delithiated samples are indicating that ligand holes are formed in Ru4d–O2p levels, which charge-compensates the extraction of Li ions from Li₂RuO₃. The XPS results implied that the electronic structures of Ru ions also varied by the formation of hole states in the hybridized bands of Ru 4d and O 2p orbitals. The shortened Ru–O distances in the delithiated samples represent increased Ru–O hybridization. The oxygen hole states created in the highly hybridized Ru4d–O2p of Li₂RuO₃ are stabilized by the strong covalent bond. Since the hole states exist stably, electrons in the O 2p orbitals can be used for charge-compensation of Li-ion extractions.

Acknowledgments

This work was partly supported by Toyota motor corporation, SUZUKI FOUNDATION and JSPS KAKENHI Grant Number 18H03929.

References

1. J. B. Goodenough and Y. Kim, *Chem. Mater.* **22** (2010) 587-603.

2. M. Oishi, K. Yamanaka, I. Watanabe, K. Shimoda, T. Matsunaga, H. Arai, Y. Ukyo, Y. Uchimoto, Z. Ogumi and T. Ohta, *J. Mater. Chem. A* **4** (2016) 9293-9302.
3. M. Oishi, C. Yogi, I. Watanabe, T. Ohta, Y. Orikasa, Y. Uchimoto and Z. Ogumi, *J. Power Sources* **276** (2015) 89-94.
4. D. Mori, H. Sakaebe, M. Shikano, H. Kojitani, K. Tatsumi, Y. Inaguma, *J. Power Sources* **196** (2011) 6934-6938.
5. S. Venkatraman, A. Manthiram, *J. Solid State Chem.* **177** (2004) 4244-4250.
6. S. J. Clark, M. D. Segall, C. J. Pickard, P. J. Hasnip, M. I. Probert, K. Rafson, M. C. Payne, *Z. Kristallogr.* **220** (2005) 567-570.
7. M. Sathiya, A. M. Abakumov, D. Foix, G. Rouse, K. Ramesha, M. Saubanère, M. L. Doublet, H. Vezin, C. P. Laisa, A. S. Prakash, D. Gonbeau, G. VanTendeloo, J.-M. Tarascon, *Nat. Mater.* **14** (2015) 230-238.
8. H. Kobayashi, R. Kanno, Y. Kawamoto, M. Tabuchi, O. Nakamura, M. Takano, *Solid State Ionics* **82** (1995) 25-31.
9. S. Sarkar, P. Mahale, and S. Mitraz, *J. Electrochem. Soc.*, **161(6)** (2014) A934-A942.
10. J. Zhou, D. Hong, J. Wang, Y. Hu, X. Xie, *Phys. Chem. Chem. Phys.* **16** (2014) 13838-13842.
11. D. Mori, H. Kobayashi, T. Okumura, H. Nitani, M. Ogawa, Y. Inaguma, *Solid State Ionics* **285** (2016) 66-74.
12. M. Sathiya, G. Rouse, K. Ramesha, C. P. Laisa, H. Vezin, M. T. Sougrati, M.-L. Doublet, D. Foix, D. Gonbeau, W. Walker, A. S. Prakash, M. Ben Hassine, L. Dupont, J.-M. Tarascon, *Nature Mater.* **12** (2013) 827-835.
13. M. Sathiya, K. Ramesha, G. Rouse, D. Foix, D. Gonbeau, A.S. Prakash, M.L. Doublet, K. Hemalatha, J.M. Tarascon, *Chem. Mater.* **25** (2013) 1121-1131.
14. M. Saubanère, E. McCalla, J.-M. Tarascon and M.-L. Doublet, *Energy Environ. Sci.* **9** (2016) 984-991.